

Modeling of Electrostatically Actuated Fluid Flow System for Mixed-Domain Simulation

T. K. Maiti^{*1}, L. Chen¹, H. Miyamoto¹, M. Miura-Mattausch^{1,2}, and H. J. Mattausch^{1,2}

¹HiSIM Research Center, Hiroshima University, Higashi-Hiroshima, Japan

²Graduate School of Advanced Sciences of Matter, Hiroshima University, Higashi-Hiroshima, Japan

Tel: +81-824247659, *E-mail: tkm@hiroshima-u.ac.jp

Abstract—Modeling of an electrically driven fluid flow system for multi-domain simulation is reported. The electrically driven actuator force is considered by an actuator component model, based on a spring-mass-damper system with force balance formulation. The fluid flow model is developed on the basis of a Kirchhoffian network which is derived from the mass transport equation. The actuator and the fluid models are coupled through equivalent circuits, leading to a consistent approach of mixed-domain system simulation. This approach is applied to design a flexible blood pumping system where the blood flow is driven by electrical organic actuators. Modeled results are compared with 2D device simulation based on the finite element method.

Keywords—Mixed-domain; actuator; fluid; compact modeling; system modeling; continuum simulation

I. INTRODUCTION

Design of a complex heterogeneous mixed-domain system is impossible without incorporating multi-physics effects into a compact model formulation [1]. The model should capture the most important properties of the system and provide an accurate behavioral approximation [2]. Continuum simulation methods such as finite difference method, finite element method, and boundary element method consider the multi-physics effect. However, those methods suffer from high computation efforts such as convergence problem, computation time, and thus face difficulty in integration with electrical circuitry for a complete system simulation [1]. In this work, we present an electrically driven fluid flow multi-physics modeling method which can be easily interfaced with electrical circuitry and takes a short period of time in simulation. The model includes properties of spring and damping forces created by electrically controlled actuators, and properties of pressure energy and volume flow rate created by the fluid flow. Electromechanical and fluid flow component formulations are coupled through a circuit network for system-level simulation [1]. We utilize the model for blood flow calculation in a system driven by electrostatic organic actuators and controlled by organic electronic circuitry [3].

II. SYSTEM DESCRIPTION AND OPERATION

A schematic view of entire fluid flow system and a cross-sectional view of the fluid flow channel are depicted in Figs. 1 (a) and (b), respectively. The fluid flow system consists of a flexible organic control circuit, organic actuators, and a flexible membrane based fluid channel. When voltage is applied on the

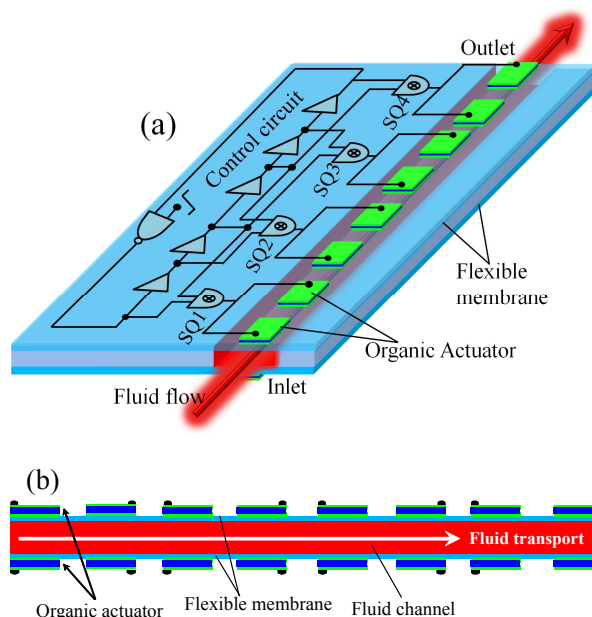


Fig. 1. (a) Illustrates a schematic view of an entire fluid flow system consisting of a control circuit, organic actuators, and a fluid channel. (b) Cross-sectional view of a fluid flow channel based on flexible membrane.

control circuit, it generates periodic driving voltage on each actuator. The positive driving voltage deflects the actuator inwards to the channel which then also bends the fluid channel membrane inwards. The inward bending of the membrane causes an underpressure inside the channel which pushes the fluid from inlet to outlet of the channel. The negative drive voltage deflects the actuator outwards which also bends the membrane outwards. The outwards bending of the membrane creates an overpressure inside the channel which causes fluid flow from outside of the system to the inside of the channel. The realization of system operation under positive and negative driving voltage, i.e., under full driving voltage cycle operation is schematically shown in Fig. 2 (a). Fluid flow path can be created by the movements of narrowing and widening of fluid channel by combining the pairs of organic actuators. The organic actuator pairs with metal electrodes can be combined to realize the fluid pumping movements as illustrated in Fig. 2(b). The described system illustrates that it is a mixed-domain system whose operation is governed by electrical, mechanical, and fluidic blocks together at a time. Fig. 3 shows a schematic

view of different domain connections through circuit networks. Computational study of such complex system using continuum simulation methods is very difficult, suffers from convergence problems, and takes long simulation time to solve. In this work, we developed compact models for each basic domain which are connected using a circuit network to perform the complete system-level simulations easily.

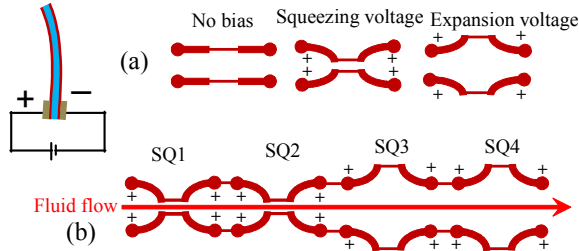


Fig. 2. (a) Operating principle of fluid-flow channel sections controlled by the actuators' driving voltage. (b) Four connected sections with two sequential squeezed and two sequential relaxed sections.

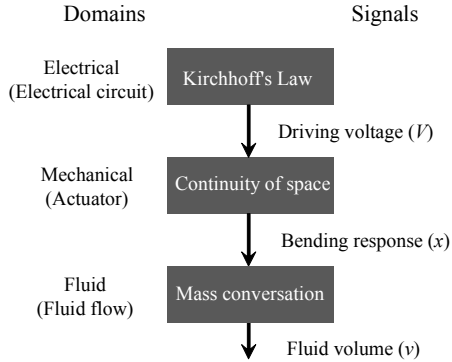


Fig. 3. Schematic of an electro-mechanical-fluidic system simulation framework with first electrical-to-mechanical and finally mechanical-to-fluid flow conversion.

III. MODEL FORMULATION AND IMPLEMENTATION

Full system simulation is done by developing compact models for each subsystem: an organic electrical control circuit, organic actuators, and a fluid flow subsystem. Each subsystem is modeled with a pair of conjugate variables consisting of force (ex: potential for electrical) and associated flow (ex: current for electrical) as an energy conservative system. The terminals of a subsystem allow the exchange of flow from one subsystem to next subsystem. General relations of force, flow, and other internal quantities in electrical, mechanical, and fluidic domains are summarized in Table 1 [1]. The interface conditions between the control circuit and the actuators are maintained *via* current flow from the electrical control circuit to the actuators by maintaining conservation of energy. The rate of change of transformation of energy, i.e., power (voltage (V) \times current (I)) from the control circuit, is equal to the driving power (Force (F) \times velocity (v)) of the actuator subsystem. Other conjugate variables such as charge (Q) and displacement (x) are also calculated from the

conservation law governing the circuit networks. Movements of actuators with velocity (v), generate pressure energy on fluid channel membranes, which interface the conditions between the actuator subsystem and the fluid subsystem through conjugate variables (fluid pressure energy (P) and fluid flow (I_f)). The electrical circuit subsystem, actuator subsystem, and fluidic subsystem are implemented in the circuit simulator using an organic thin-film transistors (OTFTs) compact model (HiSIM-Organic), an actuator compact model, and a fluid compact model, respectively, and are briefly described below.

TABLE I. GENERAL RELATION IN DIFFERENT DOMAINS (DISCIPLINES)

General	Electrical	Mechanical	Fluidic
Potential	Voltage (V)	Force (F)	Pressure (P)
Flow	Current (I)	Velocity (v)	Flow (I_f)
Displacement	Charge (Q)	Displacement (x)	Squeeze volume (V_f)
Resistance	Resistance (R)	Damper (b)	Flow resistance (R_f)
Capacitance	Capacitance (C)	Mass (m)	Fluid capacitance (C_f)
Inductance	Inductance (L)	Compliance ($1/k$)	Inertance (L_f)

A. Compact Model of the Organic Thin-Film Transistor

We designed the control circuit using the compact HiSIM-Organic model [3], [4] for OTFTs. Comparisons between HiSIM-Organic modeled (solid lines) drain current (I_{ds}) vs. gate voltage (V_{gs}) and drain current (I_{ds}) vs. drain voltage (V_{ds}) with

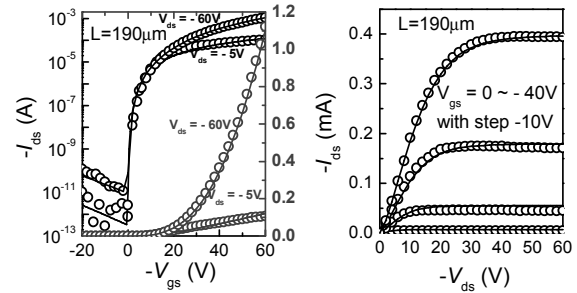


Fig. 4. Device model (solid lines) verification against measurements (symbols) for the channel length (L) of $190\mu\text{m}$. Drain current (I_{ds}) vs. gate voltage (V_{gs}) and drain current (I_{ds}) vs. drain voltage (V_{ds}) for a p-channel OTFT are shown.

measurements (symbols) for a p-OTFT are shown in Fig. 4 [5]. The model considers many important properties of OTFTs such as trap effect, floating body effect, hopping mobility, field-effect mobility, capacitance effect, leakage current effect, and contact resistance effect. The model doesn't consider the threshold voltage (V_{th}) because OTFTs device parameters such as oxide thickness (200nm), intrinsic carrier concentration (450cm^{-3}), and trap density (deep trap density = $5.0 \times 10^{17}\text{cm}^{-3}/\text{eV}$ and tail trap density $1.0 \times 10^{20}\text{cm}^{-3}/\text{eV}$) automatically determine the complete OTFTs behavior from drain current (I_{ds}) equation, which helped to design the control circuit without considering V_{th} [4]. The circuit simulations are performed with the model parameters extracted from the measurements [5]. We designed the circuit by considering the pseudo-CMOS circuit topology. Pseudo-CMOS basic circuits, such as inverter, NAND, XOR, and buffers circuits are applied to design the full control circuit.

B. Compact Model of the Organic Actuator

Electro-mechanical equivalent components of an actuator strip are schematically depicted in Fig. 5. To develop an actuator compact model, we considered an organic actuator structure which is made with an electrolytic layer placed

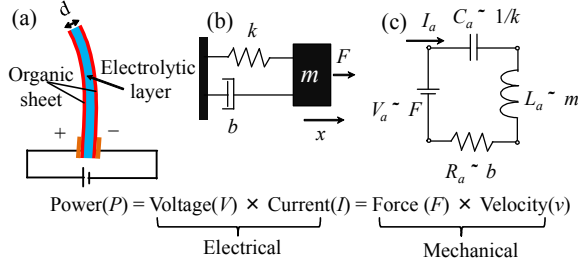


Fig. 5. (a) Illustrates a schematic diagram of an organic actuator strip, which is expressed as (b) a spring-mass-damper system with (c) an equivalent circuit element.

between two organic sheets (see Figs. 5(a) and 2) [3], [6]. From an electromechanical perspective, it behaves as a damped mass-spring system which can be actuated by electrostatic force generated *via* electrical charging and discharging of the actuator [7], [8]. Under the application of an external voltage (Fig. 6(a)), the electrolyte material is charged up and exerts an electrostatic force which is balanced by the spring-mass-damper force. Equation (1) relates the conjugate relations of electrostatic force to the mechanical force with potential (V) correspondence to force (F), resistance (R) correspondence to damping factor (b), current flow (I) correspondence to velocity (v), and charge (Q) correspondence to displacement (x).

$$\dot{x} = v, \quad \dot{v} = \frac{1}{m}(F - b\dot{x} - kx), \quad I = \frac{d}{dt}(CV) \quad (1)$$

Here, $F = \epsilon AV^2 / 2d^2$, b is the damping coefficient [8] and k is the spring constant. Above equation is implemented to describe the actuator subsystem with accounting for the analogous relations between electrical and mechanical elements as,

$$R_{\text{actuator}} \approx b, \quad L_{\text{actuator}} \approx m, \quad C_{\text{actuator}} \approx 1/k \quad (2)$$

Modeled bending responses of an actuator strip at an applied square pulse voltage of $\pm 5V$ for different values of damping

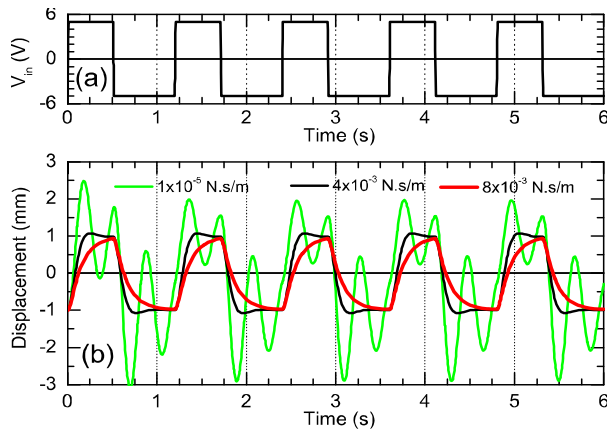


Fig. 6. (a) Periodic pulse voltage of $\pm 5V$ applied on organic actuator strip and (b) bending responses of the actuator over 6s for three different values of damping factor (see Eq. (1)) are depicted.

losses are shown in Fig. 6(b). When $+5V$ driving voltage is applied on bottom and top electrodes of the top and bottom actuators, respectively (see Fig. 2), the actuators force the membrane to squeeze which creates an inner pressure inside the fluid channel and pushes the fluid. In reverse case, when $-5V$ driving voltage is applied on the bottom and top electrodes of the top and bottom actuators, respectively, actuators bend to outwards direction of the flow channel which also moves the membrane outwards, increases the channel volume, and forces the fluid to enter this channel section. By periodic squeezing and relaxing of the channel, actuators thus drive the fluid flow.

C. Compact Model of the Fluid

Fluid flow is analogous to current flow which fulfills the Kirchhoff's network conditions as depicted in Fig. 7 [9]. We

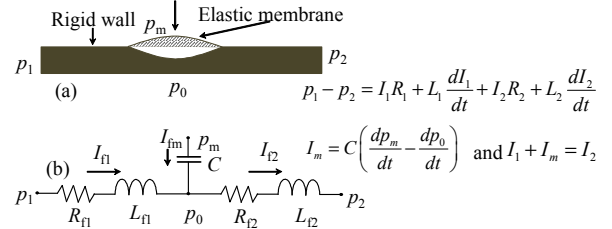


Fig. 7. (a) Implementation of Kirchhoff's network for the fluid flow is driven by squeeze membrane for one squeeze section (SQ) of Fig. 2(b). (b) Elastic membrane acts as a fluidic capacitor (C_f). Equivalent circuit with fluid resistance (R_f), capacitance (C_f), and inductance (L_f) is shown.

developed the fluid network model from the mass transport equation of fluid. Fluid resistance model (R_f) is formulated by using Bernoulli equation which is a special form of energy equation derived from Navier-Stokes equation based on mass transport theory as,

$$U = \frac{1}{\rho_f}(p + R_f I_f) \quad (3)$$

Here, U is the energy, ρ_f is the fluid density, p is the pressure of the fluid, $R_f = I_f / 2\rho_f A_f^2$, A_f is the cross sectional area of the fluid channel, and I_f is the fluid flow. The fluid capacitance (C_f) model considers the change of mass storage inside the fluid channel with the change of external pressure governed by the actuator. The fluid inductance (L_f) gives the sense of how tightly mass flows in the channel under a pressure signal. C_f and L_f are modeled using the mass transport equation. Our developed formulations for C_f and L_f are given by,

$$I_f = \rho_f k_f \frac{dP}{dt} = C_f \frac{dP}{dt}, \quad \Delta P = \frac{l_f}{A_f} \frac{dI_f}{dt} = L_f \frac{dI_f}{dt} \quad (4)$$

Here, $C_f = \rho_f k_f$, $L_f = l_f / A_f$, k_f is the fluid compressibility coefficient and l_f is the squeeze membrane length. The fluid subsystem is implemented using R_f , C_f , and L_f in a subnetwork with the conjugate pair of pressure energy (p) and fluid flow (I_f). To study the fluid flow properties through the fluid subsystem, we applied periodic triangular, sine, and square wave signals on an actuator and corresponding fluid flow responses are taken at the outlet of the channel. Fluid flow rate and total fluid flow responses are shown in Figs. 8(a) and (b),

respectively. Fig. 8 also compares the differences of fluid flow responses for triangular, sine, and square pulse signals applied on the actuator.

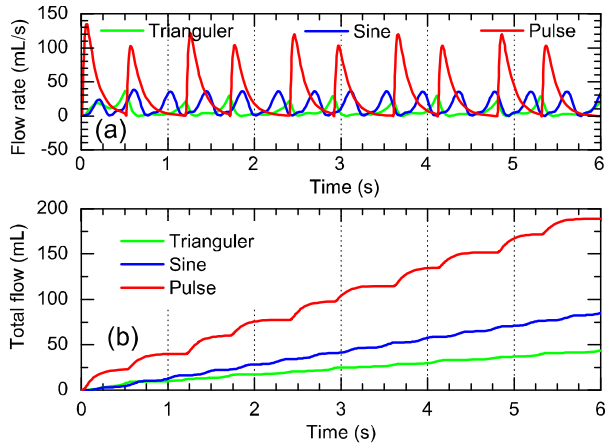


Fig. 8. (a) Responses of fluid flow driven by organic actuators. Responses are taken at the outlet of the channel for triangular, sine, and periodic pulse voltage signals applied on actuator, (b) total fluid flow.

IV. MIXED-DOMAIN SYSTEM SIMULATION

The entire electro-mechanical-fluid model is implemented in a circuit simulator using above derived sub-models which are connected according to the network shown in Fig. 1(a). Signal responses are shown together for each subsystem in Fig. 9(a). The full system simulations are done to design a blood transport system for medical application. Blood density, viscosity, and compressibility are defined as model parameters

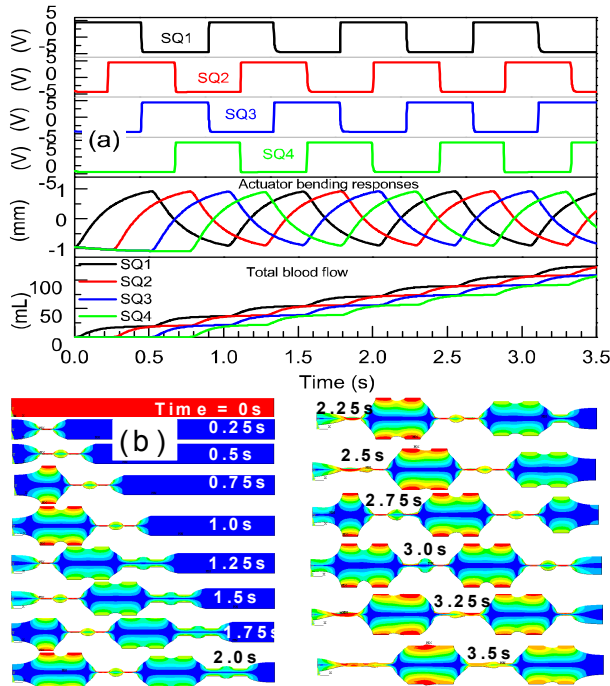


Fig. 9. (a) Signal responses at each subsystem are illustrated. (b) Simulation of membrane displacement history is shown, using finite-element-method-based 2D numerical simulation.

in the fluidic compact model. We did 2D numerical simulation using finite element method in conjunction with Arbitrary-Lagrange-Euler formulation and volume of fluid analysis to verify the model (Fig.10) [10]. Membrane displacement history obtained from numerical simulation is shown in Fig. 9(b).

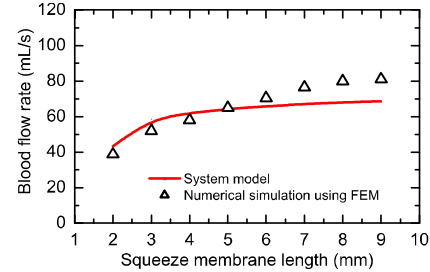


Fig. 10. Modeled results are compared with 2D numerical simulation.

V. CONCLUSIONS

We have presented an electrically actuated fluid flow system model for multi-domain simulation. Spring-mass-damper system with force-balance formulation and mass transport equation are considered to develop actuator and fluid-flow model components, respectively. Verilog-A code is used for model implementation to allow easy access by system designers. Thus a valuable tool is provided for designing and analyzing systems in which fluid flow is driven by squeezed walls which are controlled by electrostatic actuators.

REFERENCES

- [1] T. Bechtold, G. Schrag, and L. Feng, System-level Modeling of MEMS. Wiley-VCH Verlag GmbH & Co. KGaA, 2013.
- [2] D. Amsellem and J. Roychowdhury, "ModSpec: An Open, Flexible Specification Framework for Multi-Domain Device Modelling", *IEEE Int. Conf. on Computer-Aided Design (ICCAD)*, pp. 367-374, Nov. 2011.
- [3] L. Chen, T. K. Maiti, H. Miyamoto, M. Miura-Mattausch, and H. J. Mattausch, "OTFT Circuit Design for Actuator Driving Control in an Organic Fluid Pump," *46th Int. Conf. on Solid State Devices and Materials (SSDM)*, pp.908-909, Sept. 2014.
- [4] T. K. Maiti, T. Hayashi, L. Chen, H. Mori, M. J. Kang, K. Takimiya, M. Miura-Mattausch, and H. J. Mattausch, "A Surface Potential Based Organic Thin-Film Transistor Model for Circuit Simulation Verified With DNTT High Performance Test Devices," *IEEE Trans. on Semi. Manu.*, vol. 27, Iss. 2, pp.159-168, May 2014.
- [5] M. J. Kang, I. Doi, H. Mori, E. Miyazaki, K. Takimiya, M. Ikeda, and H. Kuwabara, "Alkylated Dinaphtho[2,3-b:2',3'-f]Thieno[3,2-b]Thiophenes (C_n-DNTTs): Organic Semiconductors for High-Performance Thin-Film Transistors," *Adv. Mater.*, vol. 23, Iss. 10, pp.1222-1225, March 2011.
- [6] K. Mukai, K. Asaka, T. Sugino, K. Kiyohara, I. Takeuchi, N. Terasawa, D. N. Futaba, K. Hata, T. Fukushima, and T. Aida, "Highly Conductive Sheets from Millimeter-Long Single-Walled Carbon Nanotubes and Ionic Liquids: Application to Fast-Moving, Low-Voltage Electromechanical Actuators Operable in Air," *Adv. Mater.*, vol 21, Iss. 16, pp.1582-1585, April, 2009.
- [7] S. D. Senturia, *Microsystems Design*. Norwell, MA: Kluwer Academic Publisher, 2001.
- [8] G. M. Rebeiz, *RF MEMS, Theory, Design and Technology*, Hoboken, NJ: Wiley, 2003.
- [9] H. M. Schaedel, *Fluidische Bauelemente und Netzwerke*. Vieweg-Verlag, Braunschweig, 1979.
- [10] ANSYS@Academic Research, Release 15.0, *Mechanical APDL Guide*, ANSYS Inc., 2014.